Porous Scaffolds for Bone Tissue Engineering

Subjects: Orthopedics

Contributor: Mikhail V. Kiselevskiy , Natalia Yu. Anisimova , Alexei V. Kapustin , Alexander A. Ryzhkin , Daria N. Kuznetsova , Veronika V. Polyakova , Nariman A. Enikeev

Porous structures produced from biocompatible titanium alloys using selective laser melting can present a promising material to design scaffolds with regulated mechanical properties and with the capacity to be loaded with pharmaceutical products. Adjusting pore geometry, one could control elastic modulus and strength/fatigue properties of the engineered structures to be compatible with bone tissues, thus preventing the stress shield effect when replacing a diseased bone fragment. Adsorption of medicals by internal spaces would make it possible to emit the antibiotic and anti-tumor agents into surrounding tissues. The developed internal porosity and surface roughness can provide the desired vascularization and osteointegration.

additive manufacturing | bioactive scaffolds | porous materials

1. Introduction

With recent progress in additive manufacturing (AM) technology, the number of publications on developing porous materials for biomedical applications exhibits an avalanche-alike growth, as denoted in a series of very recent extensive reviews [1][2][3][4][5]. The advantages of AM approaches to engineer fine-structured, property-controlled, and custom-designed products of numerous metallic, ceramic, carbon, and plastic materials stipulated the development of porous materials with enhanced mechanical, biocompatible, and bioactive properties. Successful exploring this area demands the realization of multidisciplinary concepts, joining efforts of prominent researchers in the field of AM technology, computer-assisted design, multiscale simulation and machine learning, tissue engineering, microstructural assessment, property characterization, biomedical studies, orthopedic surgery, and so on. Specialists from these different fields might under or overestimate the possible troubles arising from every particular aspect of developing an “ideal” final product.

2. AM Approaches to Print Porous Structures

2.1. AM Techniques to Print Porous Biocompatible Products of Ti Alloys and the Features of As-Printed Materials

3D printing is known to introduce both internal defects and geometrical deviations in the manufactured workpieces caused by the quality of powders, non-optimal processing parameters, and native peculiarities of AM technology [6]. These features may affect the functional performance of the printed articles. Achieving high-quality products requires laborious monitoring procedures involving instrumental control and computer-assisted engineering,

including machine learning [7]. Adopting AM for medical products is impossible without the implementation of specialized approaches allowing to highly precisely print defect-free, thoughtfully architectured articles.

Modern AM techniques can provide rapid prototyping of complicated 3D structures via progressive layer-by-layer joining materials programmed with the model data [8]. There are numerous AM methods, each with its own ups and downs depending on the specific application, as denoted in many comprehensive reviews [9][10][11]. It is important to note that high-precision printing of fine structures with complicated geometry is possible using AM methods based on the fusion of ultra-dispersed powders powered by laser or electron beam, which have become the most popular techniques to manufacture medical devices [1][2][3][4][5][11]. The former is often referred to as the Selective Laser Melting (SLM) technique. However, SLM represents rather a proprietary name of the AM process owned by the inventor, SLM Solutions Group AG, Lübeck, Germany. To keep the consistency, both techniques are categorized using the main prototyping principle and labeled as laser or electron beam powder bed fusion (L-PBF and EB-PBF, respectively).

PBF techniques enable the printing of porous structures with the finest available dimensions of pores (starting from 20–25 µm) [12] of high-quality biocompatible alloys. Even if modern studies predict an optimal pore size to be in the range of 300–600 µm (see below), the AM process must ensure much higher precision of printing than the designed pore dimensions. Even to compose 300 µm-sized pores, one needs to provide a printer resolution ability to reproduce geometrical features of several tens of microns. PBF techniques are capable of producing such precise porous structures with smooth surfaces [13][14][15].

Printing parameters for porous structures can significantly vary depending on the specific material and application [16]. Printing percolating porous structures with sophisticated fine-scale internal geometries demands the highest achievable precision [17] provided by using powders with the least possible particle size as well as the smallest laser beam size with corresponding accuracy of the positioning system accompanied with appropriate laser power/energy density [18][19][20].

PBF processing parameters can have a significant effect on the homogeneity of the structure and properties of printed samples, as well as provoke the formation of undesired AM-induced defects such as voids, cracks, and unmelted particles [21][22]. The location of the product on the printing platform can entail scattering in properties of the printed objects with deviations varied from 5 to 17% depending on their location [22]. High residual stresses may arise due to heterogeneous heating and rapid solidification during the PBF process, while post-printing annealing can affect the mechanical performance and phase composition of the printed articles as well as lead to the formation of cracks, shape distortion, and detachment from the supports [23][24].

The microstructure of the AM materials is usually characterized by a fine-grained structure that arises from the rapid solidification of melted metal powders. The size and morphology of the grains and fragments can vary depending on the alloy's composition, AM parameters, and heat transfer during the process [16][19][20][21]. Phase composition can also be affected by the printing processes of Ti alloys accompanied by optional precipitation of intermetallics [25]. At high cooling rates, depending on the class of a Ti alloy, a structure from a quasi-equilibrium

Widmanstett structure consisting of α-phase plate packets [26] to a non-equilibrium fine-dispersed acicular martensite structure [27] with a high density of dislocations and twins [28] can be formed out of β-phase grains. The formation of such non-equilibrium structures leads to a significant increase in the strength and a loss in ductility of printed Ti alloys compared to those produced by traditional methods of metal forming [29][30].

The aforementioned factors can influence the mechanical properties of AM-produced materials. In addition, PBF-printed specimens can exhibit a specific crystallographic texture with the preferential alignment of grains along the construction direction, which introduces considerable anisotropy of mechanical properties, especially in materials with low symmetry, such as Ti alloys [31].

The PBF 3D printing process can additionally result in heterogeneous surface roughness due to the layered deposition of material, which is important from a biomedical point of view. To improve surface quality, dedicated post-processing methods such as chemical or electrolytic etching should be used [32]. The texture and topography of the surface can affect the wettability, adhesion, and corrosion resistance of printed materials [33].

Additional trouble with the printed porous structures is related to the intrinsic feature of AM technology: unmelted particles can be trapped in the internal cavities of the printed product [34]. The presence of trapped powders is undesired for articles designed for medical applications, and cleaning by powder recovery systems is required. Standard techniques such as air jet cleaning might be insufficient to release trapped powder from porous specimens with complicated internal geometry [34], and chemical or ultrasound vibration procedures must be applied.

2.2. Computational Techniques for AM-Aimed Cell Design and Virtual Testing of Porous Structures

Bioactive scaffolds need a purposeful design of porous structures with fine, sophisticated geometry to satisfy numerous requirements of regulated mechanical properties, osteo-inductivity and conductivity, biocompatibility, permeability, and capacity for drug loading.

Understanding how the design of porous structures defines the properties of printed articles is highly important to achieving high-quality medical products with desired performance. The models of porous structures are characterized by the spatial arrangement of cells consisting of pores and inter-pore walls, the pore size and their distribution, cell geometry, configuration of inter-pore partitions, the type of pore relief, etc. [35].

At the same time, it should be noted that for the normal development of bone tissue, porous materials must provide the diffusion of fluids and nutrients, as well as the removal of metabolic waste [36][37][38]. It should also be considered that the structure of the material is important for the functioning of bone tissue during and after the process of regeneration and remodeling [39][40][41]. This subsection considers computer-aided design of the pore geometries and numerical approaches to simulate the target properties of the cellular structures.

There are various computer-aided methods to design porous materials regarding the configuration of their internal topology. They can roughly be classified as constructed with (i) spatially arranged cells composed of struts, (ii) triply periodic minimal surfaces (TPMS), and (iii) irregular bio-inspired stochastic or Voronoi tessellation structures [5][42][43][44][45][46]. The latter two techniques provide versatile capabilities to engineer porous scaffolds with controllable mechanical performance and enhanced cell colonization and proliferation [44][47]. While irregular structures mimic the natural composition of bone tissues, their design, and AM processing are laborious because of higher scattering of results among the generated structures as well as poorer basis for comparison of their performances.

Let us consider the basic principles for the computer-aided development of porous structures on the example of the most popular approach for the flexible design of versatile porous materials based on the mathematical representation of cellular structures by TPMS [47][48]. This approach provides an easy-to-implement yet powerful tool to mimic the topological, mechanical, physical, and biological properties of natural bone [48].

TPMS is an infinite and periodic curved surface that does not contain self-intersecting fragments and allows for the creation of homogeneous structures. These surfaces have crystallographic group symmetries: cubic, tetragonal, hexagonal, rhombic. TPMS is formed using an implicit method, i.e., using unambiguous functions of three variables, and the surface is defined using three axis parameters [49] (x, y, z). An example of describing a TPMS surface is an equation of the general type (1):

$$\cos \alpha x + \cos \beta y + \cos \gamma z = c,$$

where α, β, γ are parameters that determine the sizes of the base cell along the x, y, and z axes, and the constant c determines the density of the structure. That is, this equation represents a set of trigonometric functions that together satisfy the equality $\phi(x, y, z) = c$, and this function $\phi(x, y, z)$ is an isosurface evaluated by the isovalue c. Variable density, cell size gradients, hybridization, hierarchy, etc., are achieved by controlling the implicit function ($\cos(x, y, z)$ or $\sin(x, y, z)$) and the constants [50].

Currently, the most widely used programs for creating porous structures include Triangulatica, nTopology, Gen3D Sulis, Autodesk Fusion 360, Netfabb, etc., as well as the free MSLattice plugin [51], which was used to create models in MATLAB (R2022b), SpaceClaim (for ANSYS R19.1), and OpenSCAD (2021.01). **Figure 1** illustrates the opportunities to construct porous cylinders differently designed based on various models.

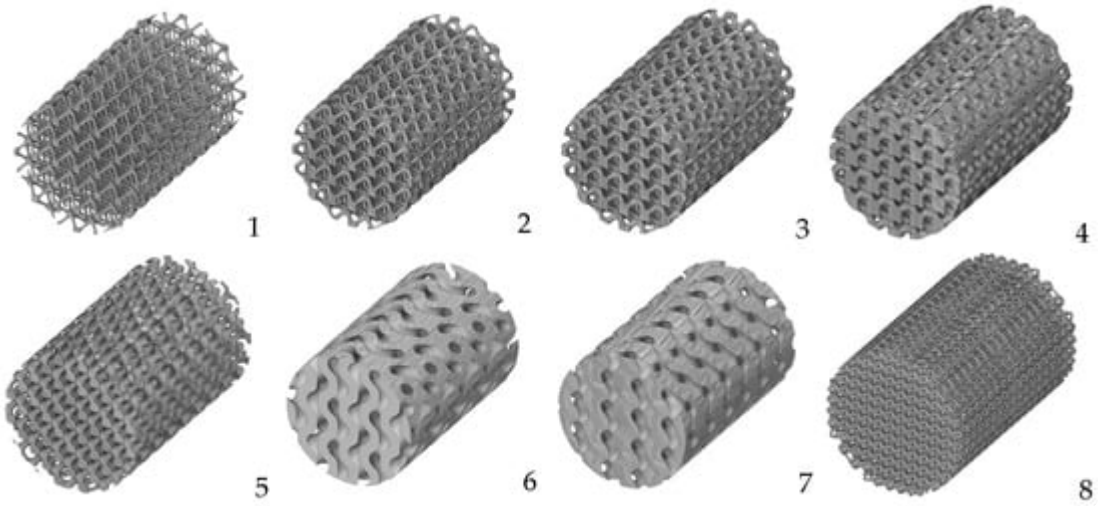

Figure 1. Models of a cylindrical sample built using TMPS models with different parameters featuring visualization of the different pore/wall ratio within IWP design (**1**–**4**) and different cell designs: Diamond (**5**) Gyroid (**6**,**7**) as well as strut-based octa-alike construction (**8**).

Important to highlight a problem related to the mismatch between the designed and printed models, which is originated from the 3D printing process listed above: heterogeneous solidification of melted powders; residual stresses, which can cause noticeable deviation of the product's geometry from the desired shape; inaccuracies associated with the finite size of the laser beam, comparable to the size of the printed pores and non-perfect positioning [1]. **Figure 2** [52] shows a comparison of the designed and printed fragments of the cellular structure, showing AM-induced inaccuracy in the reproduction of the desired cell walls. Note that the authors of [52] used very fine powders with volume-weighted equivalent diameters as small as d_{10} = 12.1 µm, d_{50} = 23.6 µm and d_{90} = 37.6 µm. A laser beam size was 30 µm to reliably print the cells with the minimal strut thickness of 100 µm.

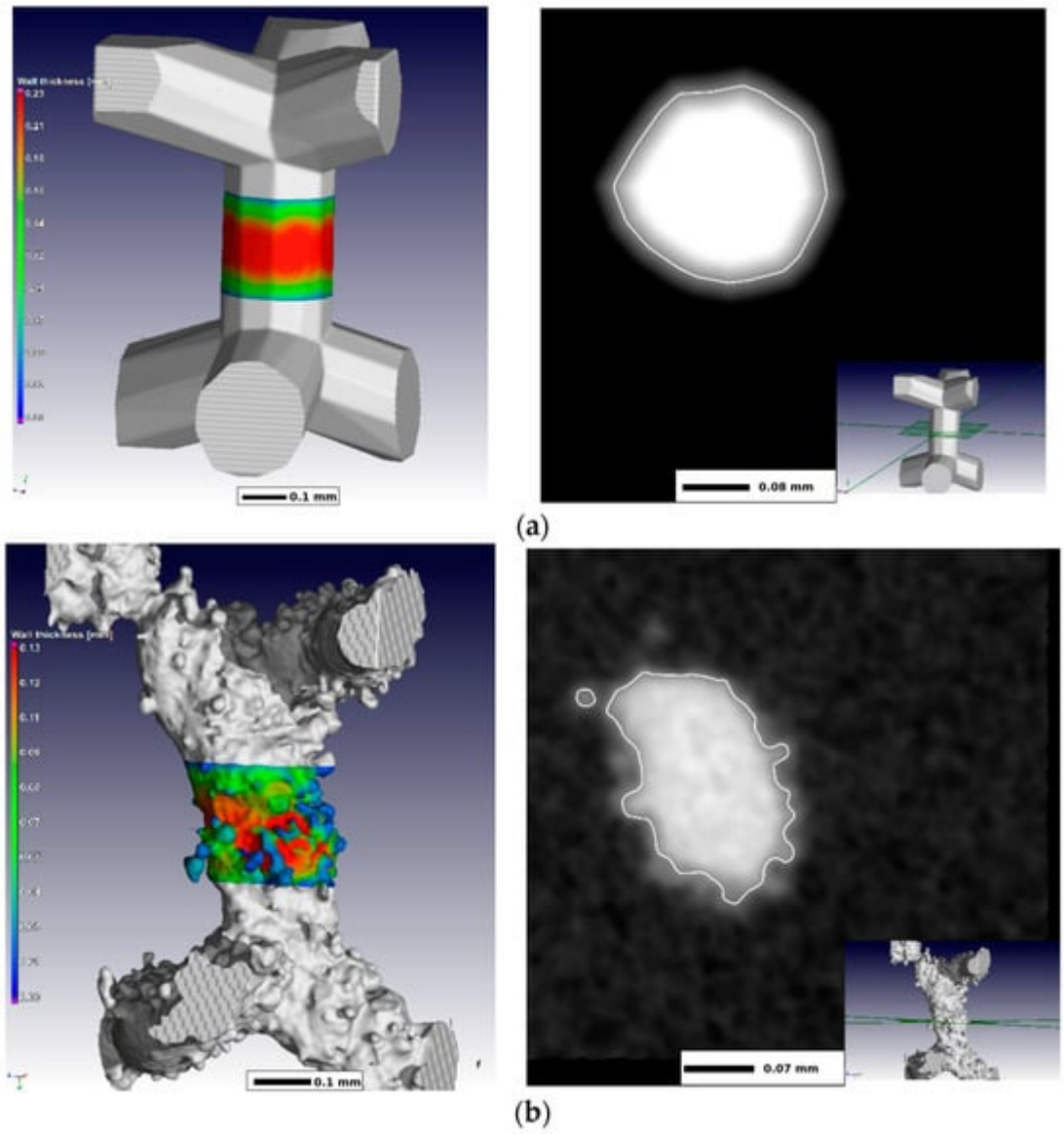

Figure 2. Micro CT images of (**a**) designed and (**b**) manufactured cell walls and their cross-sections. The figure is reproduced from [52] under the terms of the BB-CY license.

2.3. Virtual Optimization of Porous Structures for Biomedical Applications

Assuming that the studies on developing pore geometry for superior functional performance of bioactive scaffolds require optimization of the design and service properties in multi-dimensional parameter space, the application of computer simulation seems to be vital for further progress in the area. Finite-element modeling (FEM), dedicated to virtual testing of differently designed porous structures and accompanied by experimental validation, represents the most overwhelmingly growing field of study in developing bioactive implants. Numerous reviews testify that virtual testing of porous articles is able to adjust key parameters of their mechanical performance demanded by biomedical applications, such as strength, stiffness, and fatigue resistance, as well as biomedical properties [1][2][3][4][5][53]. However, high-precision computer simulations of the sophisticated internal geometry of the developed products require substantial computation power. Moreover, the mechanical response of generic porous configurations may not be calculated in full-field approximation, even using a representative volume element

approach at reasonable computational cost [54]. The limitations imposed by meshing allow us to numerically study the materials with low porosity only (less than ~20%) without pore interconnections [55]. Mean-field approximations reducing demands for computational power do not guarantee proper accuracy if complicated cases of sophisticated microstructures or non-linear behavior are considered [54][56]. Multi-scale or multi-process simulations (such as those considering fluid dynamics of drug release by porous structures) require immense computation power available in supercomputers with parallel implementations of computational tools [57]. Another major challenge for computer simulation of porous implants is presented by a problem of interrelation between their topology and biomedical properties: cell proliferation and colonization, vascularization, osteointegration, and osteoinduction, which often impose contradictory requirements to the pore geometry and the internal surfaces.

Modern computational solutions based on machine learning could significantly contribute to solving these problems. Several studies demonstrate a promising potential of artificial intelligence (AI) to optimize and predict a number of mechanical parameters such as compressive strength, tensile strength, shear, and Young's modulus [58][59]; to evaluate stress-shielding effect [60]; to design drug delivery systems [61]; to account for printing quality [62]; to mimic natural cellular and porous structures [63].

3. Porous Scaffolds for Bone Tissue Engineering: Biomedical Issues

3.1. Porous Matrices

As denoted in the chapters hereinabove, AM methods are widely used to obtain porous metallic structures, allowing for the production of materials with controlled microarchitecture. Porous biological metallic matrices built using the PBF methods have shown promising results in both in vitro and in vivo studies [64]. Porous metal scaffolds are already being used in orthopedics for the implantation of artificial joints and for the reconstruction of bone defects caused by infection, trauma, or tumor resection [65]. The porous structure can reduce risks associated with the stress shielding effect by matching the mechanical properties of the bone and promoting osteointegration in the bone-implant contact zone, providing the transport of nutrients necessary for the viability and differentiation of precursor osteocyte cells. Unlike ceramics and polymers, porous metallic materials have the advantage of balanced mechanical properties and a unique skeletal structure, which expands their application possibilities in orthopedics [66]. Metallic matrices can have a homogeneous or irregular pore size [67][68]. Homogeneous pore size allows for controlled porosity, providing predictable mechanical properties and scaffold biocompatibility [69][70]. However, the human trabecular bone does not have a consistent porosity, so homogeneous porous matrices are not optimal for cell adhesion and proliferation. On the contrary, irregular porous structures, similar to the spongy structure of bone, enhance the biocompatibility of porous matrices and are more favorable for cell growth [71][72][73]. Most non-uniform porous matrices were obtained using the reverse engineering method based on CT imaging, which allows for the simulation of the microarchitecture of natural bone [74]. The mathematical modeling method based on Voronoi-Tessellation enables the construction of approximate models of biomimetic heterogeneous porous materials [75][76]. Methods based on Voronoi-Tessellation not only optimize the microarchitecture of the

matrices but also regulate the mechanical properties (elastic modulus and compressive strength) of the porous matrices, which is important for bone tissue engineering [77].

3.2. Cell Geometry

Early studies of materials with different pore sizes have shown that the optimal pore radius for bone ingrowth is 50 µm and can reach up to 150 µm [78][79][80]. According to Lu et al., human osteoblasts can penetrate, colonize, and proliferate inside macro-pores, with a favorable size of over 40 µm [81]. Later, Itala et al. investigated laser-perforated titanium matrices with pore sizes of 50 µm, 75 µm, 100 µm, and 125 µm and found the formation of osteonal structures even in the smallest openings, leading to the conclusion that pore size within this range does not affect bone ingrowth in perforated titanium matrices [82]. Similar results have been obtained in several other studies, considering the minimal matrix pore size to be within the range of 50–100 µm [83][84]. Moreover, authors of [84] mention that osseointegration occurred even in microporosities of about 10 µm, while reducing pore size below submicrometer scale inhibits bone ingrowth. Xue et al. investigated the influence of the pore size of porous titanium on cell penetration and bone ingrowth. The results showed that porous scaffolds with a pore size of 188 µm were covered with cells, but there was a disruption in oxygen and nutrient exchange, leading to cell death within the matrix, and the optimal pore size was found to be over 200 µm [85].

Taniguchi et al. [86] reported that the PBF porous Ti6Al4V implant with a porosity of 65% and a pore size of 600 µm had comparable mechanical strength to bone, higher fixation capability, and greater bone ingrowth compared to implants with pore sizes of 300 and 900 µm. This is consistent with the recent results by Liu et al. [87] showing that the best osteogenic properties and desired mechanical performance were demonstrated by trabecular bone scaffolds characterized by 65% porosity with a pore size of 550 µm. Wieding et al. [88] concluded that a porous Ti6Al4V matrix with a pore size of 700 µm stabilized segmental bone defects in sheep tarsal bones. Li et al. [89] conducted in vitro experiments to investigate matrices with pore sizes of 500 µm, 600 µm, and 700 µm and porosities of 60% and 70%. Matrix with a size of 500 µm and a porosity of 60% demonstrated superior cell proliferation and osteogenic differentiation of rat bone marrow mesenchymal stem cells (MSCs) in vitro and bone ingrowth in vivo [90].

3.3. Biocoatings of Porous Structures

Orthobiologicals are biological substances such as bioactive molecules, stem cells, or demineralized bone grafts that are used to heal bone defects more quickly. Porous matrices made of titanium alloy, printed on a 3D printer, enhance angiogenesis, osteoblast adhesion, and promote osseointegration. However, titanium alloys are biologically inert, making the attachment between the implant and bone tissue weak. Therefore, surface treatment and implant structure must be considered in order to develop optimal porous implants. Cell differentiation and bone ingrowth are accelerated when the implant surface is covered with a bioactive material or when chemical and thermal treatments are applied, transforming the smooth titanium surface into a rough bioactive surface [91]. It has been demonstrated that chemical and thermal treatment, by immersion in a 5M aqueous solution of NaOH at 60 °C for 24 h, enhances the osteoinductive properties of porous titanium implants and does not require additional use of

osteogenic cells or bone morphogenetic protein. Thus, bioactive porous titanium could be an attractive alternative to existing orthopedic implants under load conditions [92]. There are several methods to enhance the biological activity of metallic implants through surface treatment with bioinert metals and simulated body fluid (SBF), which mimics the composition of human plasma. As a result, a biomimetic apatite coating can form on the material surface. One of them is plasma spraying of calcium phosphate, which is one of the most studied methods, and its effectiveness has been confirmed [93].

3.4. Cell Colonization

For the purposes of bone tissue engineering, MSCs are widely used due to their ability to proliferate and undergo osteogenic differentiation [94]. Titanium possesses stable biocompatibility and, according to some studies, even promotes cell adhesion and proliferation [95] (**Figure 2**). In in vitro studies, titanium mesh membranes with square openings ranging from 25 µm to 75 µm have been shown to promote cell adhesion and proliferation [96]. Functionalizing titanium via the application of bioactive coatings, particularly derivatives of hydroxyapatite, significantly enhances MSC osteogenic differentiation and angiogenesis in human umbilical vein endothelial cells [97]. Endothelial microvascular network plays an important role in osteogenesis, bone regeneration, and bone tissue engineering. Endothelial progenitor cells (EPCs) have a high angiogenic and vasculogenic potential. Colonization of EPC matrices enhances their vascularization and formation of new bone tissue.

3.5. Clinical Studies of Porous Ti-Based Materials

In a clinical study, a porous titanium interbody cage was used in patients undergoing anterior cervical discectomy to achieve interbody fusion. The titanium cages were characterized by high porosity (80%) and large pore size (700 microns) to facilitate osteointegration. The results showed that the clinical effectiveness of the titanium cages was not significantly different from that of traditionally used polyetheretherketone with (auto) graft. However, faster consolidation was observed [98].

To achieve fusion in patients undergoing anterior cervical discectomy, 3D-printed porous titanium and polyetheretherketone interbody cages with autograft were used as cervical implants. 3D-printed porous titanium cervical implants demonstrated significantly better clinical outcomes. Although there were no differences between the groups after 12 months, the titanium cages led to faster vertebral consolidation [98]. In a clinical study, 51 patients with primary osteoarthritis of the hip joint were randomized into two groups. In the experimental group, a porous titanium construct backside was implanted, while in the control group, patients were given a conventional porous coated titanium cup. When assessing periacetabular bone mineral density two years after surgery and implant fixation, no significant differences were observed between the two groups [99].

References

1. Davoodi, E.; Montazerian, H.; Mirhakimi, A.S.; Zhianmanesh, M.; Ibhadode, O.; Shahabad, S.I.; Esmaeilizadeh, R.; Sarikhanig, E.; Toorandaz, S.; Sarabi, S.A.; et al. Additively manufactured metallic biomaterials. Bioact. Mater. 2022, 15, 214–249.
2. Vesvoranan, O.; Anup, A.; Hixon, K.R. Current Concepts and Methods in Tissue Interface Scaffold Fabrication. Biomimetics 2022, 7, 151.
3. Lv, Y.; Wang, B.; Liu, G.; Tang, Y.; Lu, E.; Xie, K.; Lan, C.; Liu, J.; Qin, Z.; Wang, L. Metal Material, Properties and Design Methods of Porous Biomedical Scaffolds for Additive Manufacturing: A Review. Front. Bioeng. Biotechnol. 2021, 9, 641130.
4. Koju, N.; Niraula, S.; Fotovvati, B. Additively Manufactured Porous Ti6Al4V for Bone Implants: A Review. Metals 2022, 12, 687.
5. Du Plessis, A.; Razavi, S.M.J.; Benedetti, M.; Murchio, S.; Leary, M.; Watson, M.; Bhate, D.; Berto, F. Properties and applications of additively manufactured metallic cellular materials: A review. Prog. Mater. Sci. 2022, 125, 100918.
6. Kim, F.H.; Moylan, S.P. Literature Review of Metal Additive Manufacturing Defects; Advanced Manufacturing Series (NIST AMS); National Institute of Standards and Technology: Gaithersburg, MD, USA, 2018.
7. Li, X.; Jia, X.; Yang, Q.; Lee, J. Quality Analysis in metal additive manufacturing with Deep Learning. J. Intell. Manuf. 2020, 31, 2003–2017.
8. Mellor, S.; Hao, L.; Zhang, D. Additive manufacturing: A framework for implementation. Int. J. Prod. Econ. 2014, 149, 194–201.
9. Herzog, D.; Seyda, V.; Wycisk, E.; Emmelmann, C. Additive Manufacturing of Metals. Acta Mater. 2016, 117, 371–392.
10. Ngo, T.D.; Kashani, A.; Imbalzano, G.; Nguyen, K.T.Q.; Hui, D. Additive manufacturing (3D printing): A review of materials, methods, applications and challenges. Compos. Part B Eng. 2018, 143, 172–196.
11. Da Silva, L.R.R.; Sales, W.F.; Campos, F.d.A.R.; de Sousa, J.A.G.; Davis, R.; Singh, A.; Coelho, R.T.; Borgohain, B. A Comprehensive Review on Additive Manufacturing of Medical Devices. Prog. Addit. Manuf. 2021, 6, 517–553.
12. Ataee, A.; Li, Y.; Wen, C. A comparative study on the nanoindentation behavior, wear resistance and in vitro biocompatibility of SLM manufactured CP–Ti and EBM manufactured Ti64 gyroid scaffolds. Acta Biomater. 2019, 97, 587–596.
13. Murr, L.E. Metallurgy principles applied to powder bed fusion 3D printing/additive manufacturing of personalized and optimized metal and alloy biomedical implants: An overview. J. Mater. Res. Technol. 2020, 9, 1087–1103.

14. Gu, D.; Shi, X.; Poprawe, R.; Bourell, D.L.; Setchi, R.; Zhu, J. Material-structure-performance integrated laser-metal additive manufacturing. Science 2021, 372, eabg1487.
15. Dumpa, N.; Butreddy, A.; Wang, H.; Komanduri, N.; Bandari, S.; Repka, M.A. 3D printing in Personalized Drug Delivery: An overview of hot-melt extrusion-based fused deposition modeling. Int. J. Pharm. 2021, 600, 120501.
16. Tshephe, T.S.; Akinwamide, S.O.; Olevsky, E.; Olubambi, P.A. Additive manufacturing of titanium-based alloys—A review of methods, properties, challenges, and prospects. Heliyon 2022, 8, e09041.
17. Farazin, A.; Zhang, C.; Gheisizadeh, A.; Shahbazi, A. 3D bio-printing for use as bone replacement tissues: A review of Biomedical Application. Biomed. Eng. Adv. 2023, 5, 100075.
18. Weaver, J.S.; Heigel, J.C.; Lane, B.M. Laser spot size and scaling laws for laser beam additive manufacturing. J. Manuf. Process. 2022, 73, 26–39.
19. Keaveney, S.; Shmeliov, A.; Nicolosi, V.; Dowling, D.P. Investigation of process by-products during the selective laser melting of Ti6Al4V powder. Addit. Manuf. 2020, 36, 101514.
20. Dowling, L.; Kennedy, J.; O'Shaughnessy, S.; Trimble, D. A review of critical repeatability and reproducibility issues in powder bed fusion. Mater. Des. 2020, 186, 108346.
21. Gu, D.; Hagedorn, Y.C.; Meiners, W.; Meng, G.; Batista, R.J.S.; Wissenbach, K.; Poprawe, R. Densification behavior, microstructure evolution, and wear performance of selective laser melting processed commercially pure titanium. Acta Mater. 2012, 60, 3849–3860.
22. Barbas, A.; Bonnet, A.-S.; Lipinski, P.; Pesci, R.; Dubois, G. Development and mechanical characterization of porous titanium bone substitutes. J. Mech. Behav. Biomed. Mater. 2012, 9, 34–44.
23. Pauzon, C.; Mishurova, T.; Evsevleev, S.; Dubiez-Le Goff, S.; Murugesan, S.; Bruno, G.; Hryha, E. Residual stresses and porosity in Ti-6Al-4V produced by laser powder bed fusion as a function of process atmosphere and component design. Addit. Manuf. 2021, 47, 102340.
24. Gloaguen, D.; Girault, B.; Courant, B.; Dubos, P.-A.; Moya, M.-J.; Edy, F.; Kornmeier, J.R. Study of Residual Stresses in Additively Manufactured Ti-6Al-4V by Neutron Diffraction Measurements. Metall. Mater. Trans. A 2020, 51, 951–961.
25. Thijs, L.; Verhaeghe, F.; Craeghs, T.; Humbeeck, J.V.; Kruth, J.-P. A study of the microstructural evolution during selective laser melting of Ti–6Al–4V. Acta Mater. 2010, 58, 3303–3312.
26. Xu, W.; Brandt, M.; Sun, S.; Elambasseril, J.; Liu, Q.; Latham, K.; Xia, K.; Qian, M. Additive manufacturing of strong and ductile Ti–6Al–4V by selective laser melting via in situ martensite decomposition. Acta Mater. 2015, 85, 74–84.

27. Murr, L.E.; Quinones, S.A.; Gaytan, S.M.; Lopez, M.I.; Rodela, A.; Martinez, E.Y.; Hernandez, D.H.; Martinez, E.; Medina, F.; Wicker, R.B. Microstructure and mechanical behavior of Ti–6Al–4V produced by rapid-layer manufacturing, for biomedical applications. J. Mech. Behav. Biomed. Mater. 2009, 2, 20–32.
28. Wysocki, B.; Maj, P.; Krawczyńska, A.; Rożniatowski, K.; Zdunek, J.; Kurzydłowski, K.J.; Święszkowski, W. Microstructure and mechanical properties investigation of CP titanium processed by selective laser melting (SLM). J. Mater. Process. Technol. 2017, 241, 13–23.
29. Kruth, J.; Mercelis, P.; Van Vaerenbergh, J.; Froyen, L.; Rombouts, M. Binding mechanisms in selective laser sintering and Selective Laser melting. Rapid Prototyp. J. 2005, 11, 26–36.
30. Jin, B.; Wang, Q.; Zhao, L.; Pan, A.; Ding, X.; Gao, W.; Song, Y.; Zhang, X. A Review of Additive Manufacturing Techniques and Post-Processing for High-Temperature Titanium Alloys. Metals 2023, 13, 1327.
31. Barriobero-Vila, P.; Gussone, J.; Stark, A.; Requena, G.; Schell, N.; Haubrich, J. Peritectic Titanium Alloys for 3D Printing. Nat. Commun. 2018, 9, 3426.
32. Soro, N.; Saintier, N.; Attar, H.; Dargusch, M.S. Surface and morphological modification of selectively laser melted titanium lattices using a chemical post treatment. Surf. Coat. Technol. 2020, 393, 125794.
33. Phani Babu, V.V.; GB, V.K. A review on 3D printing process on metals and their surface roughness and dimensional accuracy. Mater. Today Proc. 2022, 64, 523–530.
34. Khrapov, D.; Paveleva, A.; Kozadayeva, M.; Evsevleev, S.; Mishurova, T.; Bruno, G.; Surmenev, R.; Koptyug, A.; Surmeneva, M. Trapped powder removal from sheet-based porous structures based on triply periodic minimal surfaces fabricated by electron beam powder bed fusion. Mater. Sci. Eng. A 2023, 862, 144479.
35. Gibson, L.J.; Ashby, M.F.; Harley, B.A. Cellular Materials in Nature and Medicine; Cambridge University Press: Cambridge, UK, 2010.
36. Olivares, A.L.; Lacroix, D. Simulation of cell seeding within a three-dimensional porous scaffold: A fluid-particle analysis. Tissue Eng. Part C Methods 2012, 18, 624–631.
37. Lutzweiler, G.; Ndreu Halili, A.; Engin Vrana, N. The Overview of Porous, Bioactive Scaffolds as Instructive Biomaterials for Tissue Regeneration and Their Clinical Translation. Pharmaceutics 2020, 12, 602.
38. Castro, A.P.; Ruben, R.B.; Gonçalves, S.B.; Pinheiro, J.; Guedes, J.M.; Fernandes, P.R. Numerical and experimental evaluation of TPMS gyroid scaffolds for bone tissue engineering. Comp. Meth. Biomech. Biomed. Eng. 2019, 22, 567–573.

39. Castilho, M.; Pires, I.; Gouveia, B.; Rodrigues, J. Structural evaluation of scaffolds prototypes produced by three-dimensional printing. Int. J. Adv. Manuf. Technol. 2011, 56, 561–569.
40. Papantoniou, I.; Guyot, Y.; Sonnaert, M.; Kerckhofs, G.; Luyten, F.P.; Geris, L.; Schrooten, J. Spatial optimization in perfusion bioreactors improves bone tissue-engineered construct quality attributes. Biotechnol. Bioeng. 2014, 111, 2560–2570.
41. Bertassoni, L.E.; Coelho, P.G. Engineering Mineralized and Load Bearing Tissues; Springer: Cham, Switzerland, 2015.
42. Alomar, Z.; Concli, F. A Review of the Selective Laser Melting Lattice Structures and Their Numerical Models. Adv. Eng. Mater. 2020, 22, 200611.
43. Maconachie, T.; Leary, M.; Lozanovski, B.; Zhang, X.; Qian, M.; Faruque, O.; Brandt, M. SLM lattice structures: Properties, performance, applications and challenges. Mater. Des. 2019, 183, 108137.
44. Zhao, Z.; Li, J.; Yao, D.; Wei, Y. Mechanical and permeability properties of porous scaffolds developed by a Voronoi tessellation for bone tissue engineering. J. Mater. Chem. B 2022, 10, 9699–9712.
45. Wu, Y.; Wang, Y.; Liu, M.; Shi, D.; Hu, N.; Feng, W. Mechanical Properties and in Vivo Assessment of Electron Beam Melted Porous Structures for Orthopedic Applications. Metals 2023, 13, 1034.
46. Alomar, Z.; Concli, F. Compressive behavior assessment of a newly developed circular cell-based lattice structure. Mater. Des. 2021, 205, 109716.
47. Yoo, D.-J. Advanced porous scaffold design using multi-void triply periodic minimal surface models with high surface area to volume ratios. Int. J. Precis. Eng. Manuf. 2014, 15, 1657–1666.
48. Bobbert, F.S.L.; Lietaert, K.; Eftekhari, A.A.; Pouran, B.; Ahmadi, S.M.; Weinans, H.; Zadpoor, A.A. Additively manufactured metallic porous biomaterials based on minimal surfaces: A unique combination of topological, mechanical, and mass transport properties. Acta Biomater. 2017, 53, 572–584.
49. Al-Ketan, O.; Abu Al-Rub, R.K. Multifunctional mechanical metamaterials based on triply periodic minimal surface lattices. Adv. Eng. Mater. 2019, 21, 1900524.
50. Liu, F.; Mao, Z.; Zhang, P.; Zhang, D.Z.; Jiang, J.; Ma, Z. Functionally graded porous scaffolds in multiple patterns: New design method, physical and mechanical properties. Mater. Des. 2018, 160, 849–860.
51. Al-Ketan, O.; Abu Al-Rub, R.K. MSLattice: A free software for generating uniform and graded lattices based on triply periodic minimal surfaces. Mater. Des. Process. Commun. 2020, 3, 205.

52. Du Plessis, A.; Kouprianoff, D.-P.; Yadroitsava, I.; Yadroitsev, I. Mechanical Properties and In Situ Deformation Imaging of Microlattices Manufactured by Laser Based Powder Bed Fusion. Materials 2018, 11, 1663.
53. Guo, A.X.Y.; Cheng, L.; Zhan, S.; Zhang, S.; Xiong, W.; Wang, Z.; Wang, G.; Cao, S.C. Biomedical applications of the powder-based 3D Printed Titanium Alloys: A Review. J. Mater. Sci. Technol. 2022, 125, 252–264.
54. Soro, N.; Brassart, L.; Chen, Y.; Veidt, M.; Attar, H.; Dargusch, M.S. Finite Element Analysis of Porous Commercially Pure Titanium for Biomedical Implant Application. Mater. Sci. Eng. A 2018, 725, 43–50.
55. Shen, H.; Brinson, L. Finite element modeling of porous titanium. Int. J. Solids Struct. 2007, 44, 320–335.
56. Campoli, G.; Borleffs, M.S.; Amin Yavari, S.; Wauthle, R.; Weinans, H.; Zadpoor, A.A. Mechanical properties of open-cell metallic biomaterials manufactured using additive manufacturing. Mater. Des. 2013, 49, 957–965.
57. Mattila, K.; Puurtinen, T.; Hyväluoma, J.; Surmas, R.; Myllys, M.; Turpeinen, T.; Robertsén, F.; Westerholm, J.; Timonen, J. A Prospect for Computing in Porous Materials Research: Very Large Fluid Flow Simulations. J. Comput. Sci. 2016, 12, 62–76.
58. Bermejillo Barrera, M.D.; Franco-Martínez, F.; Díaz Lantada, A. Artificial Intelligence Aided Design of Tissue Engineering Scaffolds Employing Virtual Tomography and 3D Convolutional Neural Networks. Materials 2021, 14, 5278.
59. Javaid, S.; Gorji, H.T.; Soulami, K.B.; Kaabouch, N. Identification and ranking biomaterials for bone scaffolds using machine learning and PROMETHEE. Res. Biomed. Eng. 2023, 39, 129–138.
60. Jafari Chashmi, M.; Fathi, A.; Shirzad, M.; Jafari-Talookolaei, R.-A.; Bodaghi, M.; Rabiee, S.M. Design and analysis of porous functionally graded femoral prostheses with improved stress shielding. Designs 2020, 4, 12.
61. Vora, L.K.; Gholap, A.D.; Jetha, K.; Thakur, R.R.; Solanki, H.K.; Chavda, V.P. Artificial Intelligence in pharmaceutical technology and Drug Delivery Design. Pharmaceutics 2023, 15, 1916.
62. Conev, A.; Litsa, E.E.; Perez, M.R.; Diba, M.; Mikos, A.G.; Kavraki, L.E. Machine learning-guided three-dimensional printing of tissue engineering scaffolds. Tissue Eng. Part A 2020, 26, 1359–1368.
63. Siegkas, P. Generating 3D porous structures using machine learning and additive manufacturing. Mater. Des. 2022, 220, 110858.

64. Warnke, P.H.; Douglas, T.; Wollny, P.; Sherry, E.; Steiner, M.; Galonska, S.; Becker, S.T.; Springer, I.N.; Wiltfang, J.; Sivananthan, S. Rapid prototyping: Porous titanium alloy scaffolds produced by selective laser melting for bone tissue engineering. Tissue Eng. Part C Methods 2009, 15, 115–124.
65. Liang, H.; Yang, Y.; Xie, D.; Li, L.; Mao, N.; Wang, C.; Tian, Z.; Jiang, Q.; Shen, L. Trabecular-like Ti-6Al-4V scaffolds for orthopedic: Fabrication by selective laser melting and in vitro biocompatibility. J. Mater. Sci. Technol. 2019, 35, 1284–1297.
66. Yang, Y.; Yuan, F.; Gao, C.; Feng, P.; Xue, L.; He, S.; Shuai, C. A combined strategy to enhance the properties of Zn by Laser Rapid Solidification and laser alloying. J. Mech. Behav. Biomed. Mater. 2018, 82, 51–60.
67. Giannitelli, S.M.; Accoto, D.; Trombetta, M.; Rainer, A. Current trends in the design of scaffolds for computer-aided tissue engineering. Acta Biomater. 2014, 10, 580–594.
68. Wang, X.; Xu, S.; Zhou, S.; Xu, W.; Leary, M.; Choong, P.; Qian, M.; Brandt, M.; Xie, Y.M. Topological design and additive manufacturing of porous metals for bone scaffolds and orthopaedic implants: A Review. Biomaterials 2016, 83, 127–141.
69. Van Bael, S.; Chai, Y.C.; Truscello, S.; Moesen, M.; Kerckhofs, G.; Van Oosterwyck, H.; Kruth, J.-P.; Schrooten, J. The effect of pore geometry on the in vitro biological behavior of human periosteum-derived cells seeded on selective laser-melted ti6al4v bone scaffolds. Acta Biomater. 2012, 8, 2824–2834.
70. Wang, Z.; Wang, C.; Li, C.; Qin, Y.; Zhong, L.; Chen, B.; Li, Z.; Liu, H.; Chang, F.; Wang, J. Analysis of factors influencing bone ingrowth into three-dimensional printed porous metal scaffolds: A Review. J. Alloys Compd. 2017, 717, 271–285.
71. Kim, T.; See, C.W.; Li, X.; Zhu, D. Orthopedic implants and devices for bone fractures and defects: Past, present and perspective. Eng. Regen. 2020, 1, 6–18.
72. Lv, X.; Wang, S.; Xu, Z.; Liu, X.; Liu, G.; Cao, F.; Ma, Y. Structural Mechanical Properties of 3D Printing Biomimetic Bone Replacement Materials. Biomimetics 2023, 8, 166.
73. Cheng, A.; Humayun, A.; Cohen, D.J.; Boyan, B.D.; Schwartz, Z. Additively manufactured 3D porous Ti-6Al-4V constructs mimic trabecular bone structure and regulate osteoblast proliferation, differentiation and local factor production in a porosity and surface roughness dependent manner. Biofabrication 2014, 6, 045007.
74. Kou, X.Y.; Tan, S.T. A simple and effective geometric representation for irregular porous structure modeling. Comput. -Aided Des. 2010, 42, 930–941.
75. Zhang, X.; Tang, L.; Liu, Z.; Jiang, Z.; Liu, Y.; Wu, Y. Yield properties of closed-cell aluminum foam under triaxial loadings by a 3D Voronoi model. Mech. Mater. 2017, 104, 73–84.

76. Honda, H.; Nagai, T. Cell models lead to understanding of multi-cellular morphogenesis consisting of successive self-construction of cells. J. Biochem. 2014, 157, 129–136.
77. Wang, G.; Shen, L.; Zhao, J.; Liang, H.; Xie, D.; Tian, Z.; Wang, C. Design and compressive behavior of controllable irregular porous scaffolds: Based on Voronoi-tessellation and for additive manufacturing. ACS Biomater. Sci. Eng. 2018, 4, 719–727.
78. Hulbert, S.F.; Young, F.A.; Mathews, R.S.; Klawitter, J.J.; Talbert, C.D.; Stelling, F.H. Potential of ceramic materials as permanently implantable skeletal prostheses. J. Biomed. Mater. Res. 1970, 4, 433–456.
79. Bobyn, J.D.; Pilliar, R.M.; Cameron, H.U.; Weatherly, G.C. The optimum pore size for the fixation of porous-surfaced metal implants by the ingrowth of bone. Clin. Orthop. Relat. Res. 1980, 150, 263–270.
80. Pilliar, R.M. Porous-surfaces metallic implants for orthopedic applications. J. Biomed. Mater. Res. 1987, 21 (Suppl. A1), 1–33.
81. Lu, J.X.; Flautre, B.; Anselme, K.; Gallur, A.; Descamps, M.; Thierry, B.; Hardouin, P. Study of porous interconnections of bioceramic on cellular rehabilitation in vitro and in vivo. Bioceramics 1997, 10, 583–586.
82. Itälä, A.I.; Ylänen, H.O.; Ekholm, C.; Karlsson, K.H.; Aro, H.T. Pore diameter of more than 100 μm is not requisite for bone ingrowth in Rabbits. J. Biomed. Mater. Res. 2001, 58, 679–683.
83. Jones, A.C.; Arns, C.H.; Hutmacher, D.W.; Milthorpe, B.K.; Sheppard, A.P.; Knackstedt, M.A. The correlation of pore morphology, interconnectivity and physical properties of 3D ceramic scaffolds with bone ingrowth. Biomaterials 2009, 30, 1440–1451.
84. Chang, B.; Song, W.; Han, T.; Yan, J.; Li, F.; Zhao, L.; Kou, H.; Zhang, Y. Influence of pore size of porous titanium fabricated by vacuum diffusion bonding of titanium meshes on cell penetration and Bone Ingrowth. Acta Biomater. 2016, 33, 311–321.
85. Xue, W.; Krishna, B.V.; Bandyopadhyay, A.; Bose, S. Processing and biocompatibility evaluation of laser processed porous titanium. Acta Biomater. 2007, 3, 1007–1018.
86. Taniguchi, N.; Fujibayashi, S.; Takemoto, M.; Sasaki, K.; Otsuki, B.; Nakamura, T.; Matsushita, T.; Kokubo, T.; Matsuda, S. Effect of pore size on bone ingrowth into porous titanium implants fabricated by additive manufacturing: An in vivo experiment. Mater. Sci. Eng. C 2016, 59, 690–701.
87. Liu, J.; Wang, R.; Gong, X.; Zhu, Y.; Shen, C.; Zhu, Z.; Li, Y.; Li, Z.; Ren, Z.; Chen, X.; et al. Ti6Al4V biomimetic scaffolds for bone tissue engineering: Fabrication, biomechanics and osseointegration. Mater. Des. 2023, 234, 112330.

88. Wieding, J.; Lindner, T.; Bergschmidt, P.; Bader, R. Biomechanical stability of novel mechanically adapted open-porous titanium scaffolds in metatarsal bone defects of sheep. Biomaterials 2015, 46, 35–47.
89. Li, F.; Li, J.; Xu, G.; Liu, G.; Kou, H.; Zhou, L. Fabrication, pore structure and compressive behavior of anisotropic porous titanium for human trabecular bone implant applications. J. Mech. Behav. Biomed. Mater. 2015, 46, 104–114.
90. Chen, Z.; Yan, X.; Yin, S.; Liu, L.; Liu, X.; Zhao, G.; Ma, W.; Qi, W.; Ren, Z.; Liao, H.; et al. Influence of the pore size and porosity of selective laser melted ti6al4v Eli porous scaffold on cell proliferation, osteogenesis and bone ingrowth. Mater. Sci. Eng. C 2020, 106, 110289.
91. Otsuki, B.; Takemoto, M.; Fujibayashi, S.; Neo, M.; Kokubo, T.; Nakamura, T. Pore throat size and connectivity determine bone and tissue ingrowth into porous implants: Three-dimensional micro-CT based structural analyses of porous bioactive titanium implants. Biomaterials 2006, 27, 5892–5900.
92. Takemoto, M.; Fujibayashi, S.; Neo, M.; Suzuki, J.; Kokubo, T.; Nakamura, T. Mechanical properties and osteoconductivity of porous bioactive titanium. Biomaterials 2005, 30, 6014–6023.
93. Habibovic, P.; Li, J.; van der Valk, C.M.; Meijer, G.; Layrolle, P.; van Blitterswijk, C.A.; de Groot, K. Biological performance of uncoated and octacalcium phosphate-coated Ti6Al4V. Biomaterials 2005, 26, 23–36.
94. Chen, C.F.; Chen, Y.C.; Fu, Y.S.; Tsai, S.W.; Wu, P.K.; Chen, C.M.; Chang, M.C.; Chen, W.M. Characterization of Osteogenesis and Chondrogenesis of Human Decellularized Allogeneic Bone with Mesenchymal Stem Cells Derived from Bone Marrow, Adipose Tissue, and Wharton's Jelly. Int. J. Mol. Sci. 2021, 22, 8987.
95. Cohen, D.J.; Cheng, A.; Sahingur, K.; Clohessy, R.M.; Hopkins, L.B.; Boyan, B.D.; Schwartz, Z. Performance of laser sintered Ti-6Al-4V implants with bone-inspired porosity and micro/nanoscale surface roughness in the rabbit femur. Biomed. Mater. 2017, 12, 025021.
96. Sakisaka, Y.; Ishihata, H.; Maruyama, K.; Nemoto, E.; Chiba, S.; Nagamine, M.; Hasegawa, H.; Hatsuzawa, T.; Yamada, S. Serial Cultivation of an MSC-Like Cell Line with Enzyme-Free Passaging Using a Microporous Titanium Scaffold. Materials 2023, 16, 1165.
97. Yuan, B.; Liu, P.; Zhao, R.; Yang, X.; Xiao, Z.; Zhang, K.; Zhu, X.; Zhang, X. Functionalized 3D-printed porous titanium scaffold induces in situ vascularized bone regeneration by orchestrating bone microenvironment. J. Mater. Sci. Technol. 2023, 153, 92–105.
98. Arts, M.; Torensma, B.; Wolfs, J. Porous titanium cervical interbody fusion device in the treatment of degenerative cervical radiculopathy; 1-year results of a prospective controlled trial. Spine J. 2020, 20, 1065–1072.

99. Salemyr, M.; Muren, O.; Eisler, T.; Bodén, H.; Chammout, G.; Stark, A.; Sköldenberg, O. Porous titanium construct cup compared to porous coated titanium cup in total hip arthroplasty. A randomised controlled trial. Int. Orthop. 2015, 39, 823–832.